Received: 6 July 2022 | Revised: 5 February 2023 | Accepted: 6 February 2023

DOI: 10.1111/jmg.12717

ORIGINAL ARTICLE

Journal of METAMORPHIC GEOLOGY WILEY

A rutile and titanite record of subduction fluids: Integrated oxygen isotope and trace element analyses in Franciscan high-pressure rocks

F. Zeb Page[1,2] | Craig D. Storey[1] | EIMF[3]

[1]School of the Environment, Geography, and Geosciences, University of Portsmouth, Portsmouth, UK

[2]Department of Geosciences, Oberlin College, Oberlin, Ohio, USA

[3]Edinburgh Ion Microprobe Facility, University of Edinburgh, Edinburgh, UK

Correspondence
F. Zeb Page, Department of Geosciences, Oberlin College, 52 W. Lorain St., Oberlin, OH, USA.
Email: zpage@oberlin.edu

Funding information
National Science Foundation, Grant/Award Numbers: EAR-1626271, EAR-1249778; Natural Environment Research Council, Grant/Award Number: IMF528/0514; Oberlin College

Handling Editor: Sarah Penniston-Dorland

Abstract

In situ oxygen analysis of garnet in eclogite and related rocks is increasingly being used to probe the composition of subduction fluids. However, in many cases, these samples contain textural signs of both fluid flow and retrograde metamorphism, some of which may take place outside the garnet stability field. In order to test the connection between polymetamorphism and fluid infiltration, rutile rimmed by titanite from high-grade tectonic blocks of the Franciscan Formation (California, USA) was analysed for oxygen isotope ratios and trace element concentrations. Zirconium concentrations in rutile yield temperatures of ~600°C for eclogite and hornblende eclogite from three well-studied localities (Junction School, Tiburon and Ward Creek). Rutile trace element concentrations are generally low and consistent with a mafic protolith. Titanite surrounding rutile has inherited much of its trace element content from rutile, and Zr-in-titanite temperatures are spuriously high. Titanite in rutile-free samples (blueschist and eclogite from Jenner beach) have similar compositions suggesting that they were formed at the expense of rutile as well. Oxygen isotope ratios from rutile and titanite in the same sample are fortuitously similar, indicating disequilibrium between these minerals, which formed at different times and temperatures but in equilibrium with the same oxygen reservoir. Rutile in blocks with garnets zoned in oxygen isotopes are generally in equilibrium with the rims rather than the cores. Slow oxygen diffusion in rutile and the low temperatures of formation require that rutile recrystallized after fluid interaction and before blueschist facies metamorphism. External fluid interaction of Franciscan eclogites took place near the peak of metamorphism.

KEYWORDS
eclogite, Franciscan, oxygen isotope, rutile, titanite, trace element

1 | INTRODUCTION

The record of fluids preserved in exhumed high-pressure metamorphic rocks is providing new and important information in the study of fluid-mediated mass transfer from the subducting slab to the sub-arc mantle (e.g., Bebout & Penniston-Dorland, 2016). One of a variety of tools that has been applied to this problem is petrographically-guided in situ analysis of oxygen isotopes in garnet (e.g., Bovay et al., 2021; Cruz-Uribe et al., 2021; Errico et al., 2013; Martin et al., 2014; Russell et al., 2013; Vho et al., 2020) and garnet and zircon (Page et al., 2014, 2019; Rubatto & Angiboust, 2015). This approach has been used to tie fluid infiltration events, where external fluids have modified a rock's oxygen isotope ratio to pressure, temperature, and time histories preserved in garnet and zircon. However, if fluid infiltration and isotopic resetting occurs outside of the garnet stability field, minerals with different pressure–temperature (P–T) stabilities and with the ability to tie a fluid record to a tectonic record are desirable.

The titanium-rich minerals rutile and titanite (sphene) are significant trace-element reservoirs in metamorphic rocks and have become important tools in petrochronology with their ability to preserve information on metamorphic temperatures through trace-element thermometry and tie them to U–Pb isotope geochronology (e.g., Kohn, 2017; Zack & Kooijman, 2017). Similar to garnet, oxygen isotope diffusion in these minerals is sluggish, and they are likely to preserve the ratios formed during crystallization, particularly at the low temperatures found in many subduction systems (Bruand et al., 2019; Moore et al., 1998; Zhang et al., 2006). Coordinated oxygen isotope and trace-element analysis of rutile has the potential to record temperature–fluid–time histories that are both overlapping, and potentially complimentary, to those preserved in garnet and zircon. In order to evaluate this new approach, we have undertaken an analysis of the oxygen isotope and trace-element compositions of compound rutile–titanite grains from blocks found at five well-studied localities in the Franciscan Formation of California (USA). In particular, we focus on samples that preserve evidence of polymetamorphism and that have been the subjects of previous ion probe studies of oxygen isotopes in garnet.

2 | FIELD RELATIONSHIPS AND SAMPLE DESCRIPTIONS

The Franciscan Formation of central and northern California, USA (Figure 1) has long provided a window into an exhumed fossil accretionary prism and is, perhaps,

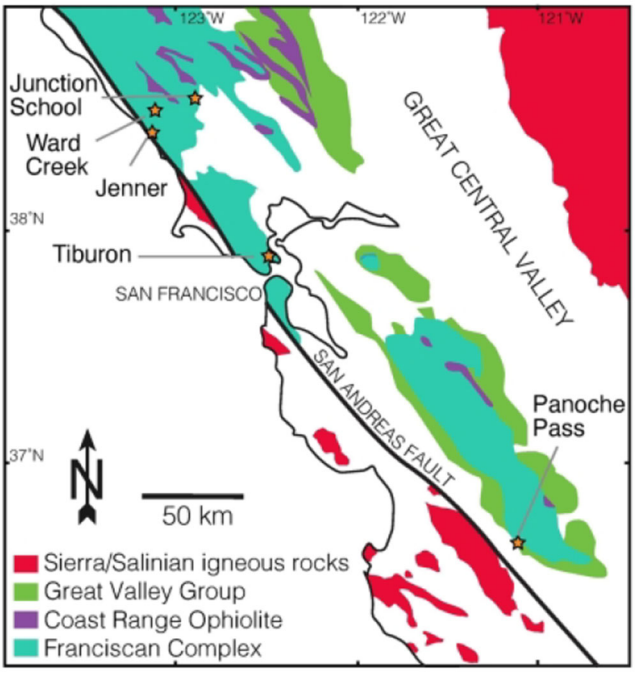

FIGURE 1 Geological sketch map of Central California, USA, showing the Franciscan Formation (after Bailey et al., 1964) and the location of the samples in this study.

the most closely studied of the circum-Pacific-type paleo subduction zones (Wakabayashi, 2015). Although a subduction origin for both the variably deformed and metamorphosed sediments and ultramafic bodies of the formation itself and the m- to dm-scale 'high-grade' tectonic blocks it hosts has become canonical (Ernst, 1970), details of field relations and mechanisms of formation remain debated (Cloos, 1982; Krohe, 2017; Wakabayashi, 2012). Much of the petrological focus on the Franciscan has been on the high-grade blocks of eclogite, plagioclase-free garnet hornblendeite and garnet blueschist that make up <<1% of the formation (Bailey et al., 1964). These blocks are commonly described as hosted by sedimentary mélanges (Ukar & Cloos, 2016); however, the majority of these blocks have obscured contacts, and many are likely no longer in situ (Raymond, 2017).

High-grade blocks are in general older and record higher temperatures than the rest of the Franciscan, and a correlation between age and temperature has been interpreted as recording a decreasing thermal gradient during the initiation of subduction (Anczkiewicz et al., 2004). However, generations of petrographers have teased out complicated histories of polymetamorphism from these blocks that require more complex tectonic mechanisms for their formation. Observations of texturally late blueschist facies minerals such as glaucophane rimming hornblende and omphacite and titanite replacing rutile are widespread throughout the Franciscan (Krogh Ravna et al., 2004;

Moore & Blake, 1989; Tsujimori et al., 2006), but omphacite is also found to replace hornblende in some samples (Essene & Fyfe, 1967) and hornblende is found to replace omphacite in others (Mulcahy et al., 2018). Moore (1984) described no fewer than three different retrograde blueschist facies events in a single tectonic block.

Rutile and titanite were analysed from nine tectonic blocks hosted by the Franciscan Formation from five sample localities: Junction School, Tiburon, Jenner, Ward Creek, and Panoche Pass (Figure 1). Below, we briefly describe the field and petrographic relationships that guided in situ isotope and trace element analysis. Sample mineralogy, International Generic Sample Numbers (IGSN) tied to location data, P–T summary and references are provided in Table 1.

2.1 | Junction School

One sample of eclogite (02H-03, IGSN:IEOMG0001) was analysed from the Junction School locality near Healdsburg (Borg, 1956; Switzer, 1945). Several dm-sized blocks rest in a field with no visible contacts, although the region is mapped as containing both sedimentary mélange and ultramafic rocks (Gealy, 1951). Detailed sample descriptions can be found in Page et al. (2007). The sample is overwhelmingly composed of garnet and omphacite, both with rutile and titanite inclusions, with minimal textural evidence of blueschist facies overprinting other than chlorite and phengite replacing some garnet rims, rare glaucophane and <100 μm rims of titanite on the abundant 200 μm to mm-scale rutile (Figure 2).

2.2 | Tiburon

Two samples of omphacite-bearing garnet-hornblende rock (commonly referred to as 'amphibolite' despite the lack of plagioclase, and referred to as hornblende eclogite in this contribution) were collected from the Ring Mountain locality on the Tiburon peninsula, north of San Francisco Bay. Blocks of eclogite, hornblende eclogite and garnet blueschist from this locality have been the subject of numerous studies detailing thermobarometry

TABLE 1 Sample descriptions and references for Franciscan tectonic blocks.

Sample	IGSN	Rock type	Mineralogy[a]	P–T conditions	Reference[b]
Junction School					
02H-03	IEOMG0001	Eclogite	Grt + Omp + Ph + Rt + Ttn ± Gln ± Chl ± Zrn ± Qz	Peak: ~20 kbar, ~550°C late: ~12 kbar, ~400°C	P07, P14
Tiburon					
02TIB-01b	IEOMG0002	Hbl eclogite	Hbl + Ep + Grt + Omp + Ph + Rt ± Ttn ± Chl ± Zrn ± Qz	Peak: ~23 kbar, ~600°C late: >7 kbar, ~350°C	W90, T06, E13
13TIB-02	IEOMG0003	Hbl eclogite	Hbl + Grt + Omp + Ph + Ep + Rt ± Ttn ± Chl ± Zrn ± Qz	"	"
Ward Creek					
02WC-01	IEOMG0004	Eclogite	Ep + Gln + Omp + Grt + Ru ± Ttn ± Chl ± Zrn ± Qz	Peak: >11 kbar, ~520°C	O91, H14, G17a, G17b
02WC-04	IEOMG0005	Eclogite	Ep + Hbl + Gln + Omp + Grt + Ttn ± Ru ± Chl ± Zrn ± Qz	"	"
02WC-08b	IEOMG0006	Eclogite	Ep + Hbl + Gln + Omp + Grt + Ttn ± Ru ± Chl ± Zrn ± Qz	"	"
Jenner					
02J-02	IEOMG0007	Blueschist	Gln + Grt + Omp + Ph + Ttn ± Chl ± Zrn ± Qz	Peak: 17 kbar, 430°C late: >11 kbar, ~350°C	K94, KT04, E13
13J-01b	IEOMG0008	Eclogite	Omp + Grt + Lws + Ph + Ttn ± Chl ± Zrn ± Qz	Peak: 17 kbar, 430°C late: >11 kbar, ~350°C	"
Panoche pass					
02PNP-05	IEOMG0009	Hornblendeite	Hbl + Grt + ep + Ap + Ilm + Ru ± Qz ± Zrn	Peak: ~700°C	P14

[a]Abbreviations after Whitney and Evans (2009).
[b]References: E13 - Errico et al. (2013), G17a - Goltz (2017), G17b - Goltz et al. (2017), H - Hoover (2014), K94 - Krogh et al. (1994), KT04 - Krogh Ravna and Terry (2004), O91 - Oh & Liou. (1990), P07- Page et al. (2007), P14 - Page et al. (2014), T06 - Tsujimori et al. (2006), W90 - Wakabayashi (1990).

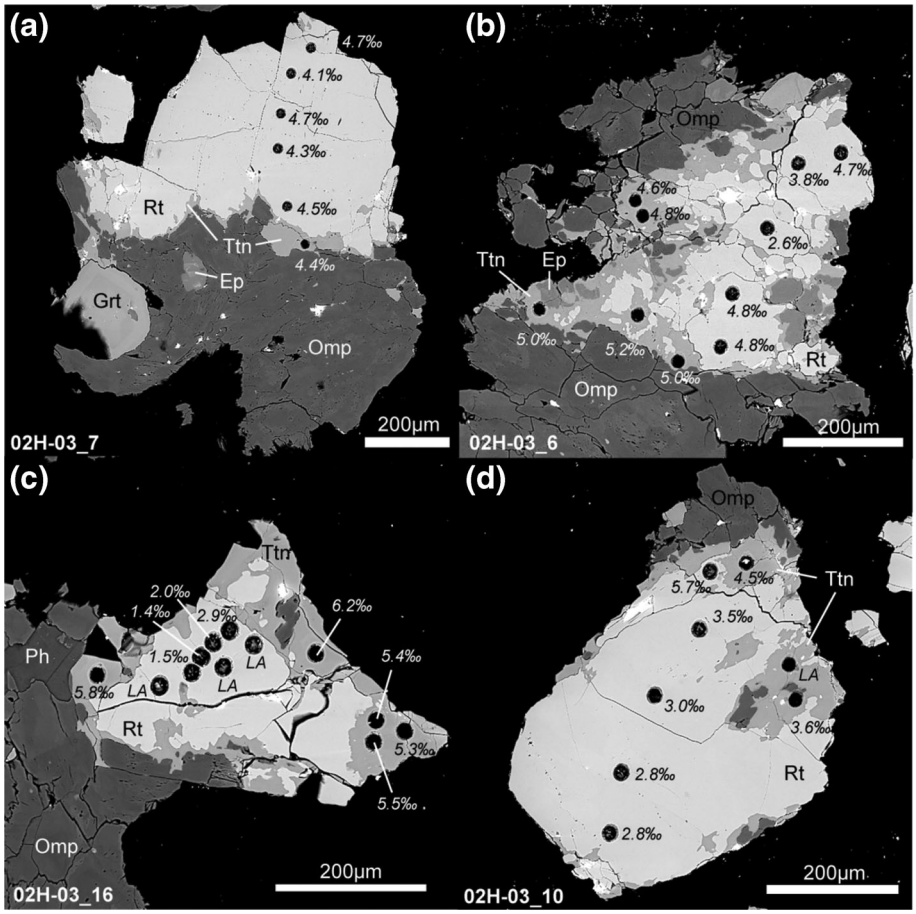

FIGURE 2 Back-scattered electron images of compound rutile-titanite grains from the Junction School eclogite with analysis locations marked by laser ablation pits from trace element analysis. Ion probe analysis pits were in the same locations as laser pits. Analysis locations are labelled with oxygen isotope ratios in $\delta^{18}O$ notation relative to VSMOW were analysed by ion probe or 'LA' were only analysed for trace elements. Mineral abbreviations follow Whitney and Evans (2009), unlabelled bright particles are remnant Au coating from ion probe analysis. (a) Typical large rutile grain, unzoned in $\delta^{18}O$ with a thin titanite overgrowth of similar $\delta^{18}O$. (b and c) rutile grains with $\delta^{18}O$ zoning, with the lowest values near the centre of the grains and homogeneous titanite rims. (d) Zoned rutile grain with high-$\delta^{18}O$ rim apparently developed on one side.

(Tsujimori et al., 2006; Wakabayashi, 1990), geochronology (Anczkiewicz et al., 2004) and whole rock chemistry and metasomatism (Horodyskyj et al., 2009). Tsujimori et al. (2006) found that hornblende-bearing blocks from Ring Mountain were metamorphosed at similar conditions to eclogite from the same locality. Both samples in this study are from blocks that rest on the shale matrix mélange of the Franciscan with obscured field relationships. The blocks have metasomatic rinds that are the result of interaction with an ultramafic host (Horodyskyj et al., 2009) and are located just downhill from the overlying ultramafic mélange that contains other blocks in situ, making it likely that they weathered out of the ultramafic unit.

Sample 02TIB-01b (IGSN:IEOMG0002) is from a m-scale block on the south side of Ring Mountain (Sample 'A' of Tsujimori et al., 2006), see that work and references therein for a detailed sample description. Abundant calcic amphiboles have glaucophane rims, and matrix 100–200 μm rutile is rimmed with titanite (Figure 3a). Garnets contain inclusions of both rutile and titanite, in addition to other minerals. Samples from Tiburon and Junction School (Section 2.1) contain texturally late white mica (associated with chlorite replacing garnet rims) that is the result of fluid metasomatism of large ion lithophile elements (LILE, Sorensen et al., 1997). Sample 13TIB-02 (IGSN:IEOMG0003) is from an hornblende-rich portion of a mixed eclogite/'amphibolite' block ('UH-12' of Horodyskyj et al., 2009). This sample has a less well-developed blueschist facies overprint with ~50 μm titanite rims on 200–300 μm rutile grains (Figure 3b).

2.3 | Ward Creek

Three samples of eclogite were collected from 'Type IV' cobbles found at the Ward Creek locality near Cazadero, California (Coleman & Lee, 1963; Oh et al., 1991). Unlike the finer-grained 'Type III' eclogite and blueschist that are found in coherent outcrop, these samples have gneissic textures and are found out of place, presumably weathered from mélange. Sample 02WC-01 (IGSN:IEOMG0004) is an euhedral garnet- and epidote-rich block with alternating glaucophane- and omphacite-rich bands. Small, <150 μm diameter, rutile grains with 10–70 μm titanite rims are found in both bands of this sample (Figure 3c,d). Sample 02WC-04 (IGSN:IEOMG0005) is an epidote-rich hornblende eclogite, containing euhedral garnets. Epidote is strongly zoned in Fe

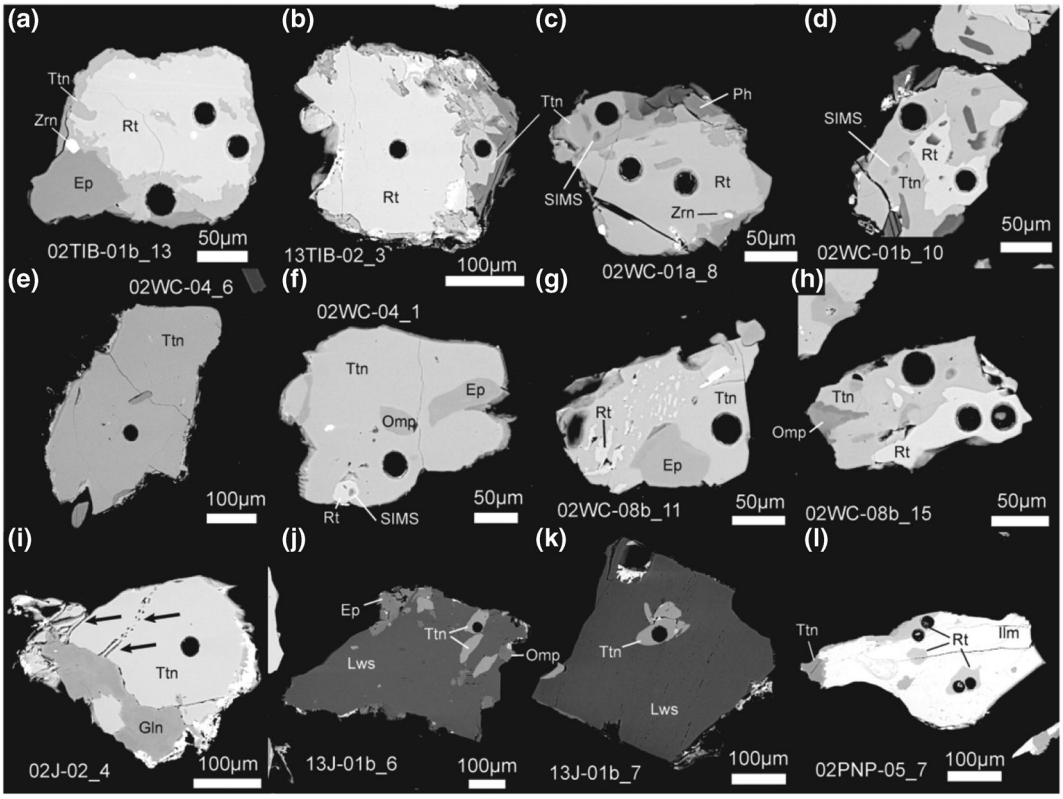

FIGURE 3 Representative back-scattered electron images of compound rutile-titanite grains from the remaining samples in this study. Analysis locations are marked by circular laser ablation pits from trace element analysis collected over previously existing ion probe pits. Mineral abbreviations follow Whitney and Evans (2009), unlabelled bright particles are remnant Au coating from ion probe analysis. (a and b) rutile grains with thin titanite rims from Tiburon hornblende eclogites. (c and d) Rutile grains with titanite rims from Ward Creek sample 02WC-01. In these grains, ion probe pits are visible adjacent to laser-ablation pits and are labelled 'SIMS'. (e) Titanite grain from Ward Creek sample 02WC-04. (f) Titanite grain from Ward Creek sample 02WC-04 containing relict rutile analysed by ion microprobe for $\delta^{18}O$, but not for trace elements. (g and h) Titanite grains from Ward Creek sample 02WC-08 with relict rutile. (i) Titanite grain from Jenner blueschist 02J-02. Arrows indicate linear TiO_2-rich features surrounded by pore-space (see text for details). (j and k) Titanite inclusions in lawsonite from Jenner eclogite 13J-01b. (l) Ilmenite grain containing rutile inclusions and a thin titanite rim from a Panoche Pass garnet hornblendite.

and Mn and occurs throughout the sample but is concentrated in bands of up to 60% epidote. Amphibole throughout the sample is zoned with calcic cores and sodic rims that are more pronounced than in the Tiburon samples. Rutile in this sample is almost entirely replaced by titanite, and exists as inclusions (alongside epidote, omphacite and glaucophane) within ~200 μm titanite grains (Figure 3e,f). More detailed sample descriptions can be found in Goltz et al. (2017) and Goltz (2017). The third eclogite from this locality, sample 02WC-08b (IGSN: IEOMG0006) has similarities to both other samples, with the exception of containing much less epidote, and having some evidence of garnet resorption. Eclogitic domains that are dominantly garnet and omphacite are interlayered with more amphibole-rich domains with abundant calcic-cored amphibole with sodic rims (Goltz & Page, 2016). As with sample 02WC-04, only relic rutile remains enclosed within 100–300 μm titanite (Figure 3g,h).

2.4 | Jenner

Numerous m-scale garnet-bearing blocks with variable amounts of glaucophane and omphacite are found below US Highway 1 and on the beach where the Russian River enters the Pacific Ocean near Jenner, California and were described in detail by Krogh et al. (1994). Recent detailed mapping of this locality by Raymond (2017) suggests that samples from the beach locality are all fragments of a single large tectonic block weathered from the overlying ultramafic mélange. We sampled two blocks from the beach with contrasting lithologies for this study. Sample 02J-02 (IGSN:IEOMG0007) is dominantly a garnet-glaucophane schist with ~cm-scale omphacite-rich domains. Sample 13J-01b (IGSN:IEOMG0008) is from a second smaller glaucophane-poor omphacite-rich block, which contains abundant mica and chlorite, replacing garnet rims. Neither of the samples contain matrix rutile.

The blueschist sample 02J-02 contains abundant 500–1000 μm titanite grains with no visible rutile, even as relicts within the titanite. Many titanite grains do contain intriguing curving linear features that appear as two parallel trenches in the mineral, up to 150 μm long and each ~1 μm wide, separated by a similar thickness of titanite (Figure 3i). There is no clear difference in back-scattered electron (BSE) contrast or composition revealed by energy dispersive X-ray analysis (EDS) between the thin ribbon of titanite and the host. Perhaps, these are remnants of fluid-pathways; however, this is speculative, and the origin of these features and their distinctive morphology remains mysterious. Titanite in the eclogite sample (13J-01b) is restricted to small (50–100 μm) inclusions in 500–1000 μm lawsonite grains (Figure 3j,k).

2.5 | Panoche Pass

Sample 02PNP-05 (IGSN:IEOMG0009) is from a dm-scale block of plagioclase- and omphacite-free garnet and brown hornblende block weathered from a serpentinite body along Panoche Pass described by Page et al. (2014). Rutile is found only as 1–40 μm round grains included in or intergrown with ilmenite (Figure 3l). Blueschist facies overprinting on this sample is primarily in the form of rare, thin rims of glaucophane on hornblende and very thin titanite rims on ilmenite grains.

3 | ANALYTICAL METHODS

Samples were crushed and sieved, and rutile/titanite composite grains from the 125–250 μm size fraction were concentrated by magnetic methods. Grains were then hand-picked under a dissecting microscope. Rutile grains from the Junction School eclogite sample were particularly large (>1 mm) and were picked directly from a lightly hand-crushed sample and mounted separately. All grains were cast in two 2.54 cm diameter epoxy disks within 5 mm of the central point. The grains were imaged in BSE using a Philips XR-30 scanning electron microscope (SEM) at the University of Portsmouth in order to evaluate compositional zoning and determine analysis locations. After ion microprobe analysis, the samples were imaged in secondary electrons (SE) in order to check pit location and morphology. Data from ion microprobe analyses that were mixtures of rutile and titanite, were on cracks, inclusions, or had 'irregular' morphologies (see Cavosie et al., 2005) were excluded. After trace element analysis on the same analytical surface and in most cases directly over the ion microprobe pit, final imaging in SE and BSE was done at Oberlin College using a Tescan Vega 3 SEM.

3.1 | Oxygen isotopes

Oxygen isotope ratios were measured on rutile and titanite at the Edinburgh Ion Microprobe Facility using a CAMECA ims1270 large-radius multi-collector ion microprobe. The instrument was tuned to an ~15 μm pit diameter using ~5 nA primary $^{133}Cs^{+}$ beam and charge compensation by a normal-incidence electron gun. The analysis pit was pre-sputtered for 40 s, and negative secondary oxygen ions were extracted at 10 kV, the beam was automatically centred in the field aperture, and $^{18}O^{-}$ (~8.0×10^{6} cps) and $^{16}O^{-}$ (~4.0×10^{9} cps) were measured simultaneously on dual Faraday cups. For the rutile data, ion probe analyses were corrected to Vienna Mean Standard Ocean Water (VSMOW) scale using the in-house PAK rutile as the primary standard reference material (SRM) with $\delta^{18}O = 2.56‰$ VSMOW, and sample-standard bracketing during the ion microprobe analysis sessions. Rutiles RAP (−1.76‰) and KAG (1.63‰) were used as secondary SRMs. All rutile SRMs were measured by conventional laser fluorination oxygen isotope analysis at the Scottish Universities Environmental Research Centre. Analytical uncertainty as defined by 2 standard deviations (2S.D.) of a set of eight standards bracketing ~10 unknown analyses ranged from 0.2 to 0.8‰. Secondary SRMs RAP and KAG were analysed as unknowns, with ion microprobe analyses reproducing their laser fluorination values within 2S.D. (Table S1) Orientation effects in rutile during SIMS analysis for U/Pb isotopes have been reported (Taylor et al., 2012), but our repeat measurements of different fragments of our SRMs (and therefore different orientations) did not yield results outside of analytical uncertainty of the expected laser fluorination values (Table S1); and so, we do not consider this potential orientation effect to have affected our results and conclusions. Titanite analyses were corrected in a two-stage process. The initial correction (assuming the same cation composition between sample and standard) was made using either Renfrew (REN, 8.49‰) or Khan Mine (KHAN, 10.51‰) titanite reference materials (Bonamici et al., 2011, 2014) as a running standard. Analytical uncertainty for each bracket ranged from 0.2 to 0.7 ‰, 2S.D. (Table S2). Solid solution of Al and Fe in titanite are a source of instrumental bias in the analysis of oxygen isotopes by ion microprobe (Bonamici et al., 2011, 2014) and were corrected for in the second step. The chemical composition of analysed titanite was measured using the Cameca SX51 electron microprobe at the University of Wisconsin–Madison

~10 μm adjacent to each ion microprobe analysis location using the same analytical procedure and formula normalization as Bonamici et al. (2014). Each ion microprobe analysis point was then corrected for compositionally-related instrumental bias using a linear relationship with Ti based on the standard materials REN, KHAN and TIBOR (Tiburon 3 titanite, −0.30‰), which range from 0.77 to 0.98 Ti atoms per formula unit (apfu). Instrumental bias curves were established for each of the three analysis sessions. Franciscan titanite samples are Fe- and Al-poor, with Ti ranging from 0.9 to 1.0 atoms per formula unit, resulting in a composition correction from the REN or KHAN SRM of up to 1.7‰.

3.2 | Trace elements

After ion probe analysis and imaging by SEM, trace elements in rutile and titanite were analysed using a New-Wave UP213 213 nm solid state Nd:YAG laser or an ASI RESOlution 193 nm ArF excimer laser coupled to an Agilent 7500cs ICP quadrupole MS at the University of Portsmouth. Samples were ablated with laser beam diameters between 20 and 40 μm, at an energy density of ~4.5 J/cm^2 and at a repetition rate of 6 Hz. In most cases, trace element analyses were performed directly over a previously analysed ion probe pit. In the rare circumstances where this was not possible, the analysis was made in the same grain as close as possible to the oxygen isotope analysis. Each analysis consisted of 20 s of background collection, 30 s of ablation, followed by a 5 s of wash-out period, resulting in a total analysis time of 55 s. Rutile was analysed for ^{27}Al, ^{29}Si, ^{45}Sc, ^{49}Ti, ^{51}V, ^{52}Cr, ^{55}Mn, ^{66}Zn, ^{69}Ga, ^{88}Sr, ^{90}Zr, ^{93}Nb, ^{95}Mo, ^{118}Sn, ^{121}Sb, ^{177}Hf, ^{181}Ta, ^{182}W, ^{208}Pb and ^{238}U. In addition to these elements, titanite was also analysed for ^{26}Mg, ^{31}P, ^{43}Ca, ^{59}Co, ^{72}Ge, ^{85}Rb, ^{89}Y, ^{137}Ba, ^{139}La, ^{140}Ce, ^{141}Pr, ^{146}Nd, ^{147}Sm, ^{151}Eu, ^{157}Gd, ^{159}Tb, ^{163}Dy, ^{165}Ho, ^{167}Er, ^{169}Tm, ^{173}Yb, ^{175}Lu and ^{232}Th. concentrations were determined using an internal standard (98 wt.% TiO_2 for rutile, Ca as analysed by electron probe for titanite) and sample-standard bracketing using NIST610 as a primary SRM (Pearce et al., 1997). Rutile SRM R10 (Luvizotto & Zack, 2009), Titanite KAHN (unpublished, in-house repository) and NIST612 (values from Jochum et al., 2011) were used as secondary standards to monitor accuracy. The measured values for all elements discussed in this paper are within 5–10% of published/known values (Table S3). A few elements reported in the Table S3 are less accurate reproduces, and are included in the Data Supplement for the sake of completion.

4 | RESULTS

4.1 | Oxygen isotopes

Oxygen isotope analyses of rutile and titanite are presented in Figure 4, and summarized in Table 2.

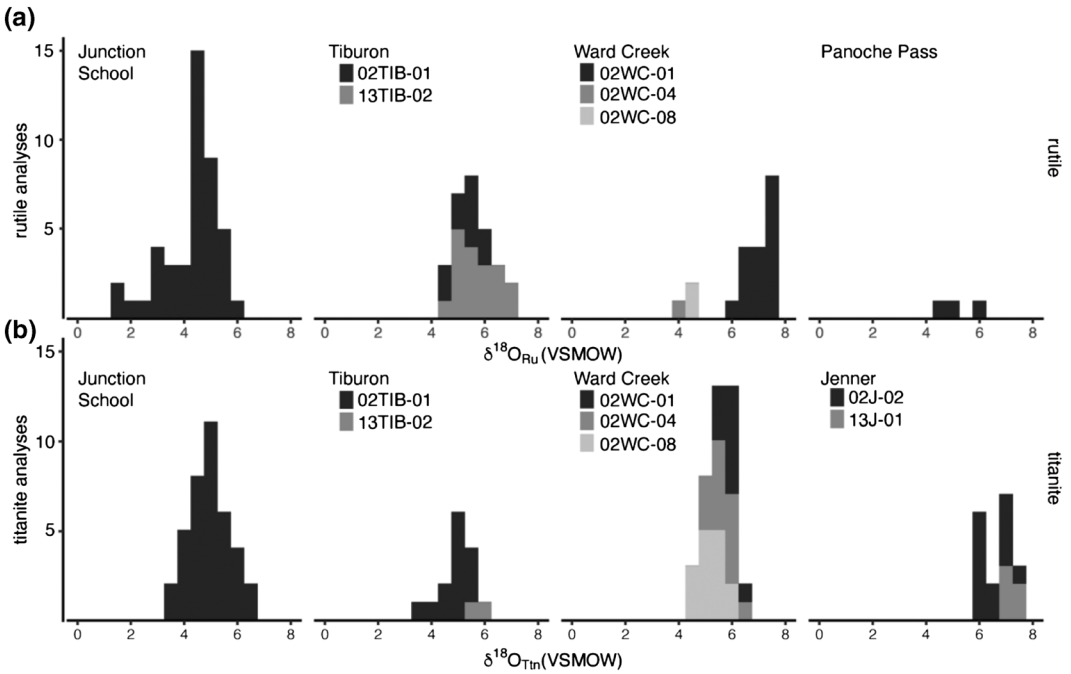

FIGURE 4 Histograms of oxygen isotope ratios in Franciscan rutile (a) and titanite (b) measured by ion microprobe. No titanite analyses were possible for the Panoche Pass sample, nor rutile analyses for the Jenner samples.

TABLE 2 Summary of $\delta^{18}O$ and [Zr] analyses of rutile and titanite from Franciscan blocks.

	Rutile										
	$\delta^{18}O$ (VSMOW)						[Zr] ppm				
Sample	Min[a]	Max[a]	Mean[a]	2S.D.	Grains	n	Min	Max	Mean	2S.D.	T °C
Junction School											
02H-03 (all)	2.0	5.7	4.2	1.9	11	44	44	123	62	19	580
"early" Ru[b]	1.4	3.5	2.6	1.5	4	10	44	93	61	28	580
"late" Ru[b]	3.7	5.9	4.7	1.1	9	34	45	74	62	15	580
Tiburon											
02TIB-01b	4.5	6.1	5.4	1.1	8	11	87	127	108	28	620
13TIB-02	4.5	6.7	5.8	1.4	13	19	66	96	82	14	600
Ward Creek											
02WC-01	6.3	8.6	7.4	1.3	24	28	39	93	70	32	590
02WC-04[c]	3.8	3.8	3.8	-	1	1	-	-	-	-	-
02WC-08b	4.6	4.7	4.6	0.4	1	2	61	61	61	-	580
Jenner											
02J-02	-	-	-	-	-	-	-	-	-	-	-
13J-01b	-	-	-	-	-	-	-	-	-	-	-
Panoche Pass											
02PNP-05	4.6	5.9	5.1	1.4	1	3	-	-	-	-	-

Abbreviation: S.D., standard deviation.
[a]Min, Max and Mean refer to individual grains per sample and are averages where grains were analysed multiple times.
[b]"early" and "late" refer to textures among grains and statistics are among analyses, not grains.
[c]Sample 02WC-04 has only one small grain of rutile.
[d]Calibration of Tomkins et al. (2007) at 20 kbar.

TABLE 2 (Continued)

	Titanite									
	$\delta^{18}O$ (VSMOW)						[Zr] ppm			
Sample	Min[a]	Max[a]	Mean[a]	2S.D.	Grains	n	Min	Max	Mean	2S.D.
Junction School										
02H-03 (all)	3.8	5.9	4.8	1.4	10	40	3	22	14	36
"early" Ru[b]	-	-	-	-	-	-	-	-	-	-
"late" Ru[b]	-	-	-	-	-	-	-	-	-	-
Tiburon										
02TIB-01b	4.0	5.5	4.9	1.0	12	14	6	11	8	3
13TIB-02	6.8	7.3	7.1	0.4	2	2	6	8	7	4
Ward Creek										
02WC-01	5.5	6.6	5.9	0.7	9	10	1	8	5	9
02WC-04[c]	5.2	6.4	5.7	0.7	12	14	22	90	38	38
02WC-08b	4.7	6.1	5.2	0.9	13	15	10	221	51	115
Jenner										
02J-02	6.0	7.2	6.5	0.9	12	13	5	205	30	117
13J-01b	6.8	7.3	7.1	0.4	5	5	5	14	9	10
Panoche Pass										
02PNP-05	-	-	-	-	-	-	-	-	-	-

Abbreviation: S.D., standard deviation.
[a]Min, Max and Mean refer to individual grains per sample and are averages where grains were analysed multiple times.
[b]"early" and "late" refer to textures among grains and statistics are among analyses, not grains.
[c]Sample 02WC-04 has only one small grain of rutile.
[d]Calibration of Tomkins et al. (2007) at 20 kbar.

Correlated analyses of oxygen isotope ratios and major and trace element analyses can be found in Table S4, and BSE images of each grain with analysis locations indicated are in Figure S5. Rutile and titanite from eclogite and hornblende eclogite from Junction School, Ward Creek and Tiburon were analysed and found to define a wide range in $\delta^{18}O$ from 1.4 to 8.6‰ (all values reported standard delta notation on the VSMOW scale). Titanite from the same samples defines a smaller but nevertheless broad range of 3.8 to 7.3‰, and, in samples with both rutile and titanite, $\delta^{18}O$ compositions overlap (Figure 4).

4.1.1 | Rutile

Samples from Junction School, Tiburon, and one from Ward Creek (02WC-01) contain abundant rutile large enough for multiple analyses. Most samples show intragrain homogeneity, although all samples show intergrain $\delta^{18}O$ values beyond analytical uncertainty. In particular, rutile from the Junction School eclogite differs from other samples as grains are both substantially larger and more heterogeneous in $\delta^{18}O$ (Figure 4). Of the 11 grains analysed, seven are homogeneous within analytical error (e.g., Figure 2a), but the other four grains display patchy zoning in $\delta^{18}O$ (Figure 2b–d). These rutile grains are not zoned in BSE imaging, and there is also no clear correlation between grain size and $\delta^{18}O$ or zoning pattern. However, domains within rutile grains preserve remnants of a low-$\delta^{18}O$ stage in this rock.

Both hornblende eclogite samples from Tiburon have overlapping rutile $\delta^{18}O$ values with variability between homogeneous grains. All three eclogite samples from Ward Creek contain rutile with titanite rims, with samples (02WC-04 and -08) preserving only minor relict rutile in titanite cores and 02WC-01 containing larger rutile grains with thinner titanite rims (Figure 3c–h). The three analyses of rutile from 02WC-04 and -08 (Table 2, Figure 4a) have lower $\delta^{18}O$ values than 02WC-01. Only three analyses of rutile (found in a single compound rutile-ilmenite grain) were possible from the Panoche Pass hornblendeite, as other rutile grains were too small to analyse using the ~15 μm diameter beam (Figure 3l).

4.1.2 | Titanite

Titanite rims from Junction School have identical isotope ratios to the more homogeneous, higher $\delta^{18}O$ rutile from that sample (Table 2, Figure 4). The similarity of these values must be fortuitous, as there is a substantial fractionation between rutile and titanite, especially at the low temperatures found in these rocks. Likewise, the $\delta^{18}O$ of titanite rims from both Tiburon samples have overlapping isotopic ratios with rutile cores. Titanite rims in sample 02TIB-01b were better developed than in sample 13TIB-02. Titanite rims from all three Ward Creek samples overlap in $\delta^{18}O$ and, collectively, show less scatter than the rutile analyses from that locale (Figure 4a,b). However, titanite from sample 02WC-01 is slightly lower than rutile from the same sample, and titanite from rutile poor samples 02WC-04 and -08b is slightly higher than the limited number of rutile analyses available from those samples.

Neither sample from Jenner was found to have rutile grains large enough to be separated for analysis. Titanite from eclogite sample 13J-01b was found primarily as inclusions in lawsonite grains. Five analyses of five ~50 μm grains yield an average of 7.1 ± 0.4‰, homogeneous within the precision of the method (Table 2, Figure 4b). Blueschist sample 02J-02 contains matrix titanite with slightly lower but overlapping values (Table 2, Figure 4b), despite differences in lithology and texture. Although thin (~1-2 μm) rims of titanite are found around some compound rutile-ilmenite grains from the Panoche Pass hornblendite, none were large enough to be analysed.

4.2 | Major and trace element composition

Rutile and titanite have substantially different crystal structures and play host to a different but overlapping cast of trace elements (Kohn, 2017; Zack & Kooijman, 2017). Zirconium concentrations are summarized in Table 2, and the full dataset is available in Table S4.

4.2.1 | Rutile

In general, trace element concentrations in rutile from Franciscan blocks are low. Rutile was not present in the Jenner samples and was too small to be analysed for trace elements in the Panoche Pass sample and Ward Creek sample 02WC-04. Grains from this study cannot be used for geochronology, with U < 1 ppm in all samples analysed. Vanadium is the most abundant trace element in these samples, followed by Nb and Cr (Figure 5a), which have been used in detrital rutile to discriminate between source rocks (Meinhold et al., 2008; Zack et al., 2004). Trace element composition is generally consistent within samples, with most samples plotting in the 'metamafic'

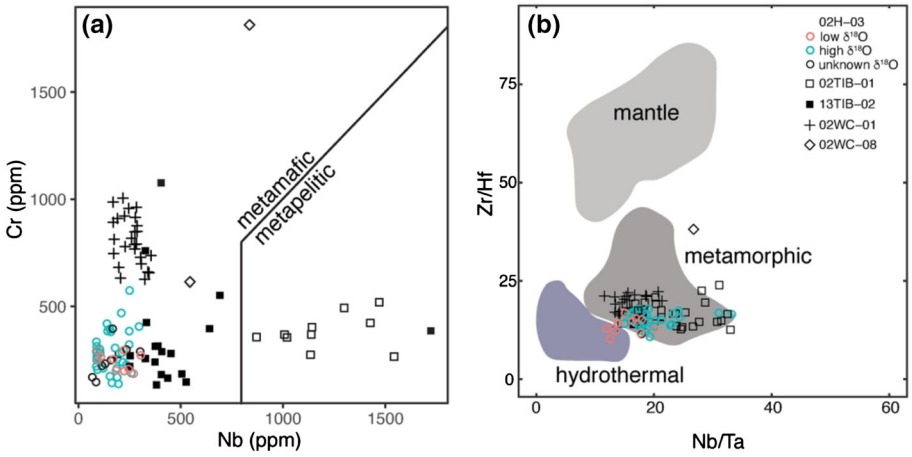

FIGURE 5 Trace-element discrimination diagrams for rutile from Franciscan blocks. (a) Cr and Nb concentrations are low and consistent with a metamafic origin for most samples (Meinhold et al., 2008; Zack et al., 2004). One Tiburon sample has slightly more elevated Nb. (b) Zr/Hf versus Nb/Ta diagram (Pereira et al., 2019).

field, and the most Nb-rich samples from Tiburon crossing the threshold into the 'metapelitic' field. The hornblende eclogites from Tiburon are clearly mafic rocks; however, the additional Nb might be from some interbedded pelitic component. Low Zr/Hf and intermediate Nb/Ta ratios are similarly consistent with a metamorphic (Pereira et al., 2019) origin for the rutile in this study (Figure 5b). Trace element analyses of low $\delta^{18}O$ rutile domains from the Junction School eclogite overlap entirely with higher-$\delta^{18}O$ zones in Cr–Nb space (Figure 5a). Low-$\delta^{18}O$ rutile from Junction School has generally lower but overlapping Nb/Ta ratios with higher-$\delta^{18}O$ rutile. Zirconium concentrations in rutile are similar among samples (Table 2), with grain averages indistinguishable at the 2S.D. level.

4.2.2 | Titanite

All samples in this study contain rutile grains with titanite rims, with the exception of the Jenner samples, where it exists as a matrix phase or inclusion in lawsonite. Titanite was analysed for major elements by electron microprobe analyser (EPMA) and trace elements by laser ablation inductively coupled plasma mass spectrometry (LA-ICPMS) for all samples but that from Panoche Pass, where titanite rims on compound ilmenite-rutile grains were too thin for analysis. All titanite was found to be very close to pure $CaTiSiO_5$. There is no F detectible by EPMA, and Ti takes up between 92 and 96% of its crystallographic site, with very minor Al > Fe substitution for Ti (Table S4). Those trace elements that are found in both rutile and titanite (e.g., Mo, Nb, Sb, Sn, Ta, V, W and Zr) have lower concentrations in titanite (Table S4). Rutile-free samples from Jenner have similarly low concentrations of most trace elements.

Unlike rutile, the crystal structure of titanite can accommodate trace levels of the rare earth elements (REE). Concentrations of REE in titanite can be found in the Table S4 and are presented as chondrite-normalized patterns in Figure 6. Titanite from those samples with well-developed rims on rutile (e.g., Ward Creek sample 02WC-08b and Junction School) have a wide range of REE compositions; patterns range from a 'hump-shaped' morphology with REE increasing in normalized concentration from La to Dy, with the heavy REE (HREE) having a slightly negative slope from Dy to Lu. In some analyses, HREE remain flat and elevated. As is commonly the case with plagioclase-free samples, Eu-anomalies are poorly developed. In contrast, the two samples from Tiburon have very low REE concentrations and patterns with a generally positive trend with increasing atomic number, with HREE enriched relative to the other elements (Figure 6b). Additionally, several analyses of sample 02TIB-01 display a negative Eu-anomaly. The two samples from Jenner beach have contrasting REE patterns (Figure 6f). Although both samples are depleted in the HREE and do not have Eu-anomalies, the shape of the patterns from Gd to Lu differ considerably. Eclogite sample 13J-01 (titanite inclusions in lawsonite) has a similar shape to samples from Junction School and Ward Creek. Blueschist sample 02J-02 has a steep negative slope from Gd to Er but, unusually, has a flat or even slightly positive slope from Er–Lu.

5 | DISCUSSION

5.1 | Trace elements

The low trace element concentrations in rutile and titanite from Franciscan blocks are consistent with their mafic protoliths and the low temperatures of their metamorphism. Rutiles analysed from these samples are generally quite similar in their trace element content, with most samples containing less than 500 ppm of even

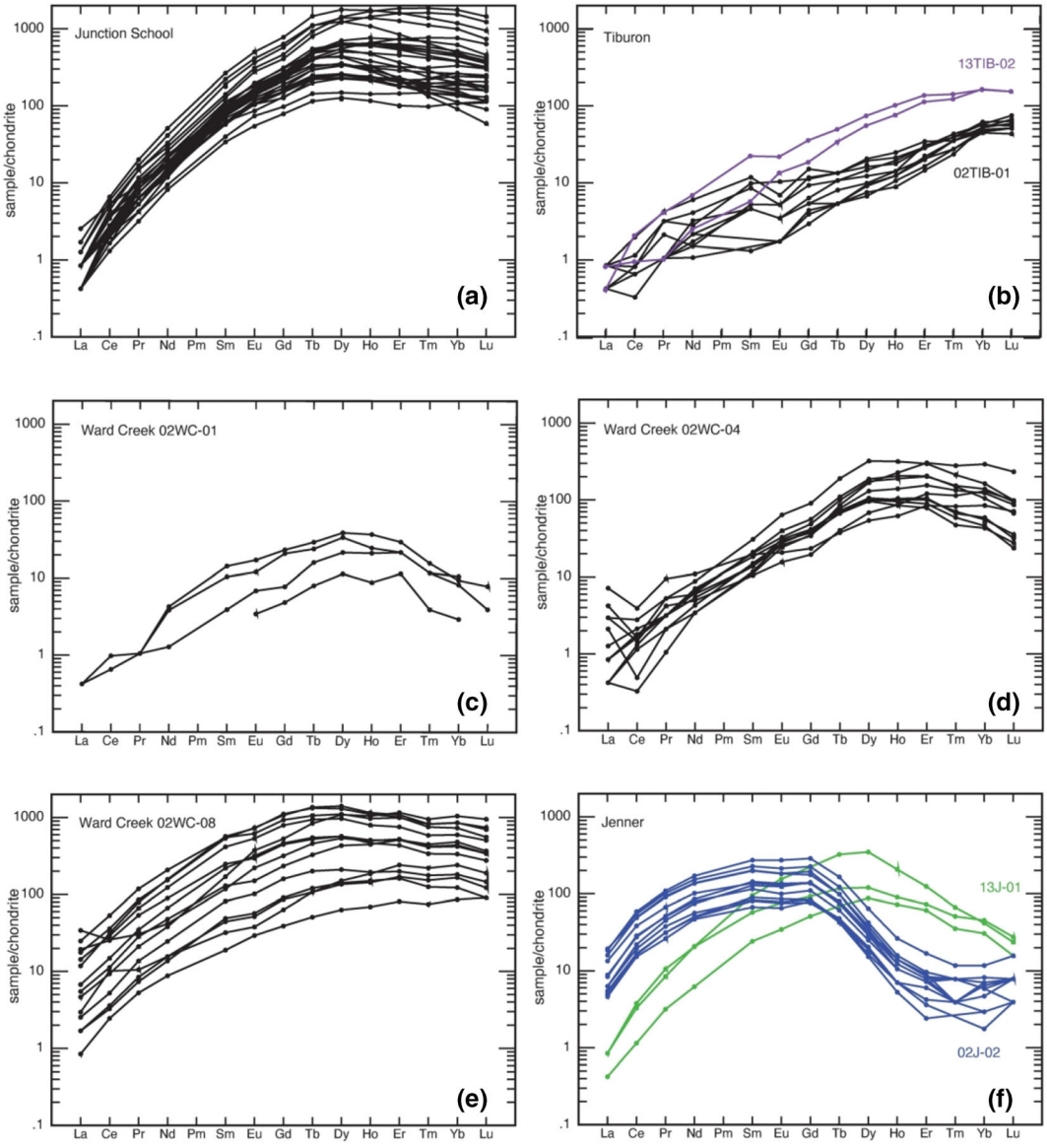

FIGURE 6 Chondrite-normalized rare earth element diagrams of titanite from Franciscan blocks.

abundant trace elements (e.g., Cr and Nb), which commonly range up to 9000 ppm and above in some lithologies (e.g., Pereira et al., 2019).

Titanite trace element concentrations (particularly REE) are similarly low in these samples when compared with igneous titanite (e.g., Kohn, 2017) or metasedimentary titanite (e.g., Garber et al., 2017; Walters et al., 2022), although there is significant variability both within and among samples (Figure 6). Three general patterns can be found in these REE diagrams and can be tied to mineralogy and lithology (eclogite, hornblende eclogite and garnet blueschist).

All samples described as eclogite in Table 1 (dominantly garnet and omphacite from Junction School, Ward Creek and Jenner sample 13J-01; Figure 6a,c–f) have similar REE patterns with a maximum around Dy and variably flat to negatively-sloped HREE. Although a changing slope in HREE (e.g., Figure 6a) is sometimes correlated with core-rim zonation in garnet as the growth of that mineral depletes the rock's available reservoir of those elements (e.g., Cruz-Uribe et al., 2021; Konrad-Schmolke et al., 2008, 2022), the variability in these samples are found among grains rather than within them. These titanites formed during a blueschist facies overprinting of eclogite, which included chlorite and phengite replacement of garnet rims (e.g., Krogh et al., 1994; Oh et al., 1991; Page et al., 2007; Sorensen et al., 1997; Tsujimori et al., 2006). Variability in HREE concentrations among these samples can be explained by variable garnet resorption, with elevated and flat HREE patterns in titanite in more retrogressed samples (e.g., Ward Creek sample 02WC-08 with slightly resorbed garnet and poorly-preserved rutile) and those with more depressed HREE (e.g., 02WC-01) found in samples with euhedral garnets

and less well-developed titanite rims. That said, titanite in all eclogite samples, but in particular the Junction School sample, has a range of HREE concentrations. The Junction School eclogite also has variably retrogressed garnets (Page et al., 2007; Sorensen et al., 1997). Given the low temperatures of the titanite formation and sluggish diffusion, proximity to dissolving garnet may also exert a strong control on the availability of trace elements to neoformed titanite. In situ analysis with petrographic context preserved is needed to test this hypothesis.

Hornblende eclogites from Tiburon (Figure 6d) have positive slopes from LREE to HREE, without the clear maximum around Dy. The presence of substantial hornblende that predates titanite growth may be responsible for the lack of enrichment in MREE; however, this does not explain the positive slope throughout the HREE in these garnet-bearing rocks. Garnet dissolution during titanite growth may, again, have been the source of HREE for these minerals (Sorensen et al., 1997).

The REE patterns for the Jenner blueschist sample 02J-02 (Figure 6f) are dramatically HREE-depleted, when compared with all other samples in this study. Limited garnet resorption or limited HREE in garnet rims is one possible explanation.

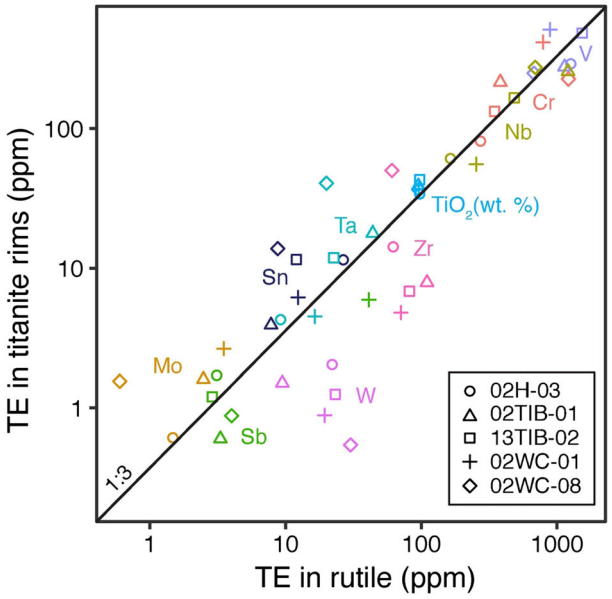

FIGURE 7 Trace elements in rutile and titanite rims for five blocks of Franciscan eclogite, hornblende eclogite and blueschist. Different trace elements are identified by colour labels, and are consistent with a 1:3 dilution with the formation of titanite at the expense of rutile (cf. Cruz-Uribe et al., 2018).

5.1.1 | Relationship between rutile and titanite

Titanite rims in this study appear to have formed as products of a rutile-out reaction. The major and trace element composition of titanite formed at the expense of rutile must come from a combination of inheritance from rutile (e.g., Ti, HFSE) and external sources (e.g., Si, Ca and Sr, REE). Given that the concentration of titanium in rutile is diluted by a third (on an atom basis) when it reacts to form titanite, one might expect (in a closed system) that the trace elements inherited from rutile by titanite would be likewise diluted (Cruz-Uribe et al., 2018). A comparison of the shared trace element concentrations in rutile and its titanite rims is consistent with this trend for the Franciscan samples (Figure 7).

5.1.2 | Zirconium thermometry

Zirconium concentrations in both rutile and titanite can be used to estimate crystallization temperatures. All samples in this study contain both matrix zircon and quartz, ensuring that the operative substitution reactions are fully buffered. Zirconium concentrations in rutile are similar among samples (61–108 ppm) and yield a relatively narrow Zr-in-rutile temperature range of 580–620°C using the calibration of Tomkins et al. (2007) and a pressure estimate of 2.0 GPa (Table 2). Peak temperature estimates for those rutile-bearing samples with existing thermobarometry closely match these temperatures within the 25–50°C uncertainties of these methods (e.g., 550–620°C, Tiburon, Tsujimori et al., 2006; 550°C, Junction School, Page et al., 2007). The agreement between trace element thermometry of rutile, a phase belonging to the presumed peak metamorphic assemblage and other thermometric techniques applied to peak phases (e.g., garnet and omphacite) provides robust evidence for maximum temperatures in the Franciscan eclogite.

As demonstrated in the previous section (5.1.1) and Figure 7, the Zr content of titanite rims on rutile is consistent with inheritance from the rutile precursor, suggesting that the use of the Zr-in-titanite thermometer is unlikely to yield meaningful temperatures. Zirconium concentrations of 5–51 ppm yield temperatures of ~700–1000°C using the Hayden et al. (2008) calibration at an estimated pressured of 1.0 GPa. These extreme temperatures are above the hottest estimates for the Franciscan and certainly inconsistent with the blueschist facies overprint. It seems far more likely that the inherited Zr from precursor rutile was unable to diffuse out of the neoformed titanite, leading to spurious temperatures (Cruz-Uribe et al., 2018). Interestingly, titanite in the rutile-free samples from Jenner also have high Zr, yielding the same extreme temperatures (Table 2). It is likely that that the titanite in these samples is a result of the complete conversion of rutile to titanite at low temperatures.

5.2 | Oxygen isotopes

A number of Franciscan eclogites have been shown to contain multiple generations of titanite, with inclusions of that mineral common in the cores of garnets as well as rimming rutile in the matrix (Oh et al., 1991; Tsujimori et al., 2006). Garnet blueschist with no rutile from Jenner also contains titanite in the matrix and as inclusions in garnet (Krogh et al., 1994). Garnets from the Junction School eclogite contain inclusions of both rutile and titanite in their cores and preserve textural evidence of two periods of garnet resorption followed by regrowth. The innermost of these garnet rims records blueschist pressures and temperatures, and the outermost contains rutile inclusions (Page et al., 2007). Most of the rocks in this study include petrologic evidence of both rutile and titanite equilibrium with garnet and, in some cases, prograde equilibrium between rutile and titanite (Junction School, Page et al., 2007). In the following sections, we examine equilibrium among rutile, titanite and garnet using in situ analyses of oxygen isotope ratios.

5.2.1 | Rutile and titanite disequilibrium

Casual inspection of Figure 4 shows that titanite $\delta^{18}O$ values are quite similar to rutile $\delta^{18}O$ values for samples with titanite rimming rutile. Average $\delta^{18}O$ values for both minerals are identical at the 2S.D. level for the Junction School sample, both Tiburon samples and all Ward Creek samples but 02WC-04. This similarity must be fortuitous as the titanite texturally post-dates the rutile and had the two minerals formed in equilibrium, the titanite should be ~1.4‰ greater in $\delta^{18}O$ value than the rutile (based on a formation temperature of 600° and fractionation factors from Matthews, 1994; Valley et al., 2003). Using the recent collection of fractionation factors by Vho et al. (2019), the titanite is predicted to be 2.0‰ greater at the same temperature. The most likely explanation is that the two minerals formed in equilibrium with the same whole rock $\delta^{18}O$ at different times and at different temperatures. For example, the $\delta^{18}O$ of rutile is 2.6‰ less than almandine garnet at 600°C (Valley et al., 2003), whereas the same fractionation between titanite and almandine is predicted at ~330°C (Valley et al., 2003). Although this latter temperature is well outside the calibration range, the temperatures cited are consistent with current temperature estimates for eclogite metamorphism and subsequent blueschist facies overprint on blocks hosted by the Franciscan, as well as the Zr in rutile temperatures from this study (Tables 1 and 2). Given that titanite commonly forms disequilibrium textures with rutile related to low-temperature blueschist overprinting of eclogite, one might actually expect fortuitously similar values of $\delta^{18}O$ based on their differing fractionation factors and a 200–300°C difference in temperatures of formation.

5.2.2 | Rutile and garnet equilibrium

The samples in this study were chosen because they contain garnets that record a history of external fluid interaction. Previous ion microprobe analyses of these garnets record a change in $\delta^{18}O$ in garnet rims (Errico et al., 2013; Goltz, 2017; Hoover, 2014; Page et al., 2014). In order to compare garnet data with rutile (or titanite for Jenner samples), ion probe analyses of garnet from literature sources were combined with Zr-in-rutile temperatures (if available, Table 2) or temperatures from the literature to calculate rutile or titanite $\delta^{18}O$ values in equilibrium with garnet using the Valley et al. (2003) fractionation factors (Figure 8).

The Junction School eclogite has low-$\delta^{18}O$ (~4.5‰) garnet cores with thin, high-$\delta^{18}O$ (~6.5‰) rims (Page et al., 2014). This sample also has a bimodal distribution in oxygen isotope ratios in rutile, with patches of low-$\delta^{18}O$ values (1.5–3.5‰) in some grains (Figure 2). The lowest-$\delta^{18}O$ rutile compositions are in equilibrium with garnet core compositions as are the bulk of the high-$\delta^{18}O$ (3.7–5.9‰) rutile analyses with garnet rims (Figure 8a). Despite the substantial overlap, average rutile isotope ratios are systematically higher that those predicted by garnet compositions, and the distinction between rutile domains is not texturally clear. Zircons in this sample are likewise zoned in $\delta^{18}O$ with cores broadly in equilibrium with low-$\delta^{18}O$ rutile domains and garnet cores and rims in equilibrium with garnet rims and also high-$\delta^{18}O$ rutile domains (Page et al., 2014). Thus, zircon, garnet and rutile in this sample record two different episodes in this rock's $\delta^{18}O$ history: an early low-$\delta^{18}O$ period and a later high-$\delta^{18}O$ stage caused by external fluid interaction, all predating the formation of titanite rims on rutile grains.

Hornblende eclogite from Tiburon contains garnet zoned in $\delta^{18}O$, but without the evidence of resorption boundaries or sudden shifts in cation zoning found in hornblende-free eclogite both at the same locality and in others. Instead, garnets show gradual zoning in $\delta^{18}O$ from ~9‰ cores to ~6‰ rims. Rutile from two Tiburon samples have a similar range in $\delta^{18}O$ to the garnets, and their isotope ratios are broadly in equilibrium with garnet, although slightly shifted to higher $\delta^{18}O$ (Figure 8a). Rutile from this locality is much smaller than the Junction School rutile, and individual grains are unzoned. The range in $\delta^{18}O$ values may be recording a gradual introduction of an external fluid into these blocks in parallel to garnet and rutile growth (e.g., Errico et al., 2013).

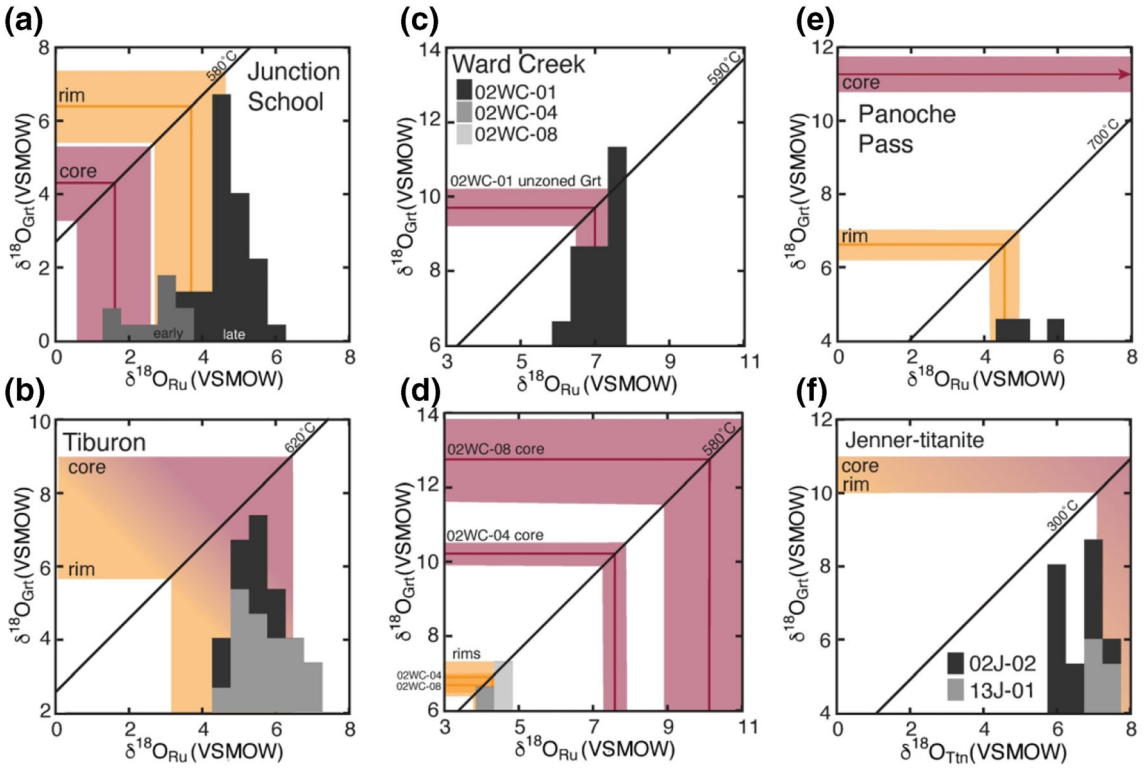

FIGURE 8 Hybrid oxygen isotope δ-δ plots and histograms to assess equilibrium between garnet and rutile or titanite in Franciscan eclogite. Literature data for garnet ion probe analyses of $\delta^{18}O$ (y-axis) are combined with Zr-in-rutile thermometry and fractionation factors (Valley et al., 2003) to calculate $\delta^{18}O$ values of rutile (or titanite) in equilibrium with garnet (diagonal 1:1 line labelled with average Zr-in-rutile T). $\delta^{18}O$ histograms (see Figure 4 for y scale) are superimposed for comparison. (a) Equilibrium rutile compositions calculated from Junction School eclogite garnet cores (average ± 2SD) overlap with low-$\delta^{18}O$ rutile domains; whereas, garnet rim compositions overlap primarily with high-$\delta^{18}O$ rutile domains. (b) Broadly-zoned Tiburon hornblende eclogite garnets (full range from Errico et al., 2013) overlap with most rutile analyses. (c) Unzoned garnet from sample 02WC-01 is in equilibrium with matrix rutile. (d) Garnet core compositions for samples 02WC-04 and 02WC-08 are far from equilibrium with matrix rutile; whereas, garnet rim compositions (similar for both samples) are in equilibrium with the limited number of matrix rutile analyses. (e) Rutile from the Panoche Pass garnet hornblendeite is in equilibrium with garnet rims, high-$\delta^{18}O$ garnet cores are in equilibrium with rutile compositions off-scale to the right. The temperature for equilibrium calculation is from Anczkiewicz et al. (2004). (f) Titanite from Jenner overlaps with the low range of equilibrium values calculated from garnet and a reference temperature from Krogh-Ravna et al. (1994).

The three eclogite samples from Ward Creek have contrasting mineralogy, $\delta^{18}O$ garnet zoning profiles and rutile $\delta^{18}O$ values. Sample 02WC-01 retains the most rutile, with only thin titanite rims and also contains unzoned garnet with a $\delta^{18}O$ composition of ~10‰ (Goltz, 2017; Goltz et al., 2017; Hoover, 2014). At the temperatures predicted with the Zr-in-rutile thermometer, the garnet $\delta^{18}O$ is in equilibrium with the rutile (Figure 8c). Samples 02WC-04 and -08 are more glaucophane-rich than sample 02WC-01, have limited amounts of relict rutile found within matrix titanite and also have garnets zoned in oxygen isotope ratios. Garnet cores are elevated in $\delta^{18}O$ relative to rims which are both ~7‰ (Goltz, 2017; Goltz et al., 2017; Hoover, 2014). Only three analyses of rutile from these samples were possible, but all of them are in equilibrium with garnet rims (Figure 8d).

The garnet hornblendeite block from the Panoche Pass region has minimal titanite overprinting on compound ilmenite-rutile grains and garnets with zoning in oxygen isotopes (~11‰ cores, ~7‰ rims, Page et al., 2014). There is no published thermometry from this block; however, garnet hornblendite from nearby (Hermes, 1973) has a peak T estimate of ~700°C (Anczkiewicz et al., 2004). As with most samples in this study, oxygen isotope ratios of rutile from this block are consistent with formation in equilibrium with garnet rims, as opposed to cores (Figure 8e).

Eclogite and garnet blueschist from Jenner beach contain titanite, not rutile. Garnet in eclogite from Jenner was analysed for oxygen isotopes by Errico et al. (2013) and was found to have limited zoning (11‰ core and 9–10‰ rims). Zr-in-titanite temperatures were found to be

unreasonably high for all samples in this study (Section 6.1.2). However, Krogh et al. (1994) estimated the conditions of the blueschist facies overprint on this block at ~300°C. Titanite $\delta^{18}O$ values from both Jenner samples are broadly in equilibrium with garnets at this temperature (Figure 8f). The range in $\delta^{18}O$ of titanite in these samples is broader than that found in garnets, so it is not possible to distinguish between equilibrium with garnet cores or rims.

In summary, rutile in blocks with sharp oxygen isotope zoning profiles in garnet rims (Junction School, Ward Creek samples 02WC-04 and -08 and Panoche Pass) is in oxygen isotope equilibrium with garnet rims and not cores. Of these, only the Junction School sample, which has by far the largest rutile grains, preserves evidence of some rutile domains in equilibrium with garnet cores. In the Ward Creek sample with no oxygen isotope zoning in garnet (02WC-01), rutile is in equilibrium with garnet cores. Samples from Tiburon hornblende eclogite have gradual zoning profiles in garnet, which is broadly in equilibrium with rutile. Likewise, titanite from the Jenner samples appears to be generally in equilibrium with garnet.

One possibility that must be considered is that matrix rutile formed originally in equilibrium with garnet cores (as one might expect from the petrography of the samples) and its oxygen isotope composition was subsequently modified by intracrystalline diffusion. However, diffusive resetting is not supported by the metamorphic setting (and thus temperatures) nor the textures found in these samples. Although the Junction School eclogite has by far the largest rutile grains in this study, there is little textural consistency to the preservation of low-$\delta^{18}O$ domains. Although the low-$\delta^{18}O$ zones are sometimes near the centre grains (e.g., Figure 2b), the lowest $\delta^{18}O$ rutile is found in a smaller grain that does appear to have some zoning, but certainly not a full diffusion profile. However, the best argument against diffusive resetting of rutile $\delta^{18}O$ is the low temperatures found throughout the Franciscan. Oxygen diffusion in rutile is quite slow, and even 50 μm grains have closure temperatures of 629°C, above the temperatures recorded by Zr-in-rutile thermometry in this study (Moore et al., 1998). If the higher-$\delta^{18}O$ composition of the ~500 μm diameter rutile in Figure 2a were the result of complete diffusional resetting at a peak temperature of 600°C, it would have required 10^8–10^9 years (Moore et al., 1998). The young age and cold thermal regime of these rocks are more consistent with recrystallization of rutile after fluid interaction than the alternative explanation.

5.3 | Tectonic and fluid implications

The integration of rutile and garnet oxygen isotope histories of eclogite blocks from the Franciscan reveals complicated records of fluid infiltration and metamorphism with differences and commonalities among different blocks. Figure 9 provides a schematic overview of the different histories preserved in the garnet and rutile-bearing blocks in this study.

Rutile trace element chemistry (Figure 5) and previous studies (e.g., Horodyskyj et al., 2009) point to a mafic (most likely oceanic basalt) protolith for the rocks in this study. Hydrothermal alteration of oceanic basalts shifts their oxygen isotope ratio from that of the mantle to

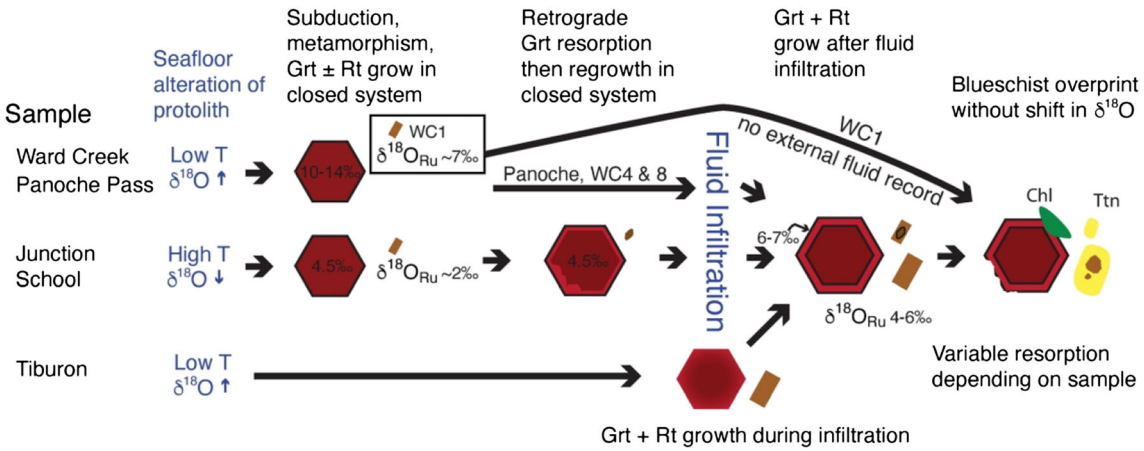

FIGURE 9 Schematic timeline of fluid and metamorphic events of rutile-bearing samples in this study. Most samples (Ward Creek, Panoche Pass and Tiburon) record elevated $\delta^{18}O$ from the low-T alteration of their protolith; whereas, Junction School garnets record the low-$\delta^{18}O$ high-T alteration. One Ward Creek sample (WC1) does not preserve evidence of fluid infiltration; whereas, all other samples do. The Junction School eclogite experienced and additional period of resorption and garnet regrowth at low-T prior to infiltration. The Tiburon sample has more gradual $\delta^{18}O$ zoning of garnet consistent with growth during infiltration (Errico et al., 2013). All samples with garnets zoned in $\delta^{18}O$ converge on similar garnet rim values. Late blueschist overprinting post-dates fluid infiltration. Mineral abbreviations follow Whitney and Evans (2009).

elevated $\delta^{18}O$ values in the case of low temperature alteration and lower $\delta^{18}O$ values in the case of high temperature alteration (Gregory & Taylor, 1981). Most garnet cores in Franciscan eclogite have elevated $\delta^{18}O$ (~10–14‰, Figure 8) consistent with subduction metamorphism of the (more abundant) low-T altered crust; whereas, only the Junction School eclogite has $\delta^{18}O$ below mantle values, likely due to a high-T alteration of the protolith (Figure 9). Garnet cores from Junction School, Ward Creek and Panoche Pass appear to have grown initially in a closed system with no change in garnet $\delta^{18}O$; whereas, garnets from Tiburon and Jenner samples record a lower-$\delta^{18}O$ infiltration during garnet growth (Errico et al., 2013). Only the Junction School sample and Ward Creek sample 02WC-01 preserve rutile from this stage (Figures 8a,c and 9). Sample 02WC-01 is the only eclogite in this study that does not record an external fluid infiltration. The other Ward Creek eclogites and Panoche Pass samples record an external fluid infiltration in both garnet rims and matrix rutile (Figure 9).

The most straightforward explanation for these data is that external fluid introduction took place near the peak of metamorphism (in the garnet and rutile stability fields, Figure 9). The formation of titanite in the blueschist facies overprinting of Franciscan high-grade blocks was not contemporaneous with the fluid interaction recorded in garnet rims but must have post-dated it, despite evidence of LILE metasomatism associated with the blueschist facies stage (Sorensen et al., 1997). This is consistent with the models proposed by Errico et al. (2013) for Tiburon and Jenner but not for Junction School, which has blueschist facies garnet rims that formed before external fluid infiltration (Page et al., 2014). Recent work on other eclogite samples from the Franciscan has tied cycles of resorption and regrowth in garnet rims to fluid overpressure and release during subduction (Viete et al., 2018). This fluid release mechanism would not introduce a contrasting isotopic signature into the rock and so must operate independently of the high-pressure fluid interaction recorded here. Rutte et al. (2020) have proposed the rapid initial exhumation of Franciscan eclogites due to the subduction of a spreading ridge, perhaps this shift in the local stress regime also allowed in introduction of an external fluid with contrasting $\delta^{18}O$ while still within the stability fields of garnet and rutile.

The Junction School eclogite has textural evidence of resorption in garnet prior to rim growth, suggesting that it moved in and out of the garnet stability field either through physical motion along the subduction interface or through changing bulk composition through metasomatism. Given that garnets were resorbed before external fluid infiltration, a metasomatic explanation is unlikely. Garnet rims have a lower Mg# after resorption boundaries, suggesting the resumption of garnet growth at a lower temperature (in contrast to the samples described by Viete et al., 2018) Garnet rims in the Junction School eclogite record blueschist facies conditions in between two different resorption boundaries, both of which precede the shift in $\delta^{18}O$ due to external fluid infiltration and most matrix rutile growth (Page et al., 2007, 2014). These data suggest that the Junction School eclogite moved out of the garnet stability field twice: the first time without interaction with external fluids but returning to it at lower temperatures and the second time after fluid interaction and with recrystallization of matrix rutile at peak T (Figure 9). The most plausible mechanism for such a convoluted history is multiple episodes of subduction through cycles of uplift and burial within a flowing subduction channel (e.g., Blanco-Quintero et al., 2011).

Despite these clear differences and complexities, there are significant commonalities among different eclogite (and related) blocks in the Franciscan, including the consistent temperatures recorded by rutile in this study, similar pressures recorded by quartz inclusions in garnet (Cisneros et al., 2022) and perhaps a similar shared early exhumation history (Rutte et al., 2020). Most garnet and rutile that formed after fluid infiltration point to a similar fluid composition in the subduction channel (Figures 8 and 9), resulting in $\delta^{18}O_{Grt} = 6–7‰$ and $\delta^{18}O_{Rt} = 4–6‰$, regardless of the initial $\delta^{18}O$. The consistency of the external infiltrating fluid across tens of kilometres (Figure 1) is evocative of the widespread homogeneous $\delta^{18}O$ fluids of the Catalina Schist (Bebout & Barton, 1989).

The three eclogite samples from Ward Creek provide something of a microcosm of the Franciscan overall, with adjacent blocks containing both zoned and unzoned garnet. Sample 02WC-01 does not record external fluids in either garnet or rutile $\delta^{18}O$, but samples 02WC-04 and -08 do. Likewise, garnet from some Jenner blocks have rims zoned in $\delta^{18}O$, whereas others do not (Errico et al., 2013). This may reveal varying scales of pervasive fluid infiltration versus channelized flow within the subducting slab (e.g., Bovay et al., 2021). It seems likely that the flow of high-grade blocks within mélange during later stages of exhumation leads to different histories as blocks potentially disaggregate, are exposed to different channelized fluid pathways and move (physically, and perhaps chemically) into and out of different mineral stability fields. Differences in fluid histories among different blocks need to be tied to pressure, temperature and time information in order to better decipher their complex histories, establish commonalities and explain contrasting

behaviours. The application of correlated trace element and oxygen isotopic analyses to rutile and titanite offers a new and complimentary lens through which these phenomena are studied.

ACKNOWLEDGEMENTS

Page gratefully acknowledges financial support from Oberlin College (Ohio, USA) and the National Science Foundation (NSF) (grants EAR-1249778 and EAR-1626271). SIMS analysis of oxygen isotopes was funded by a Natural Environment Research Council (NERC) ion microprobe facility grant (IMF528/0514). John Fournelle assisted with the electron microprobe analyses; Stephanie Lasalle assisted with ICP-MS analyses; Nigel McMillion prepared the thin sections used in this study, and the authors gratefully acknowledge the comments from Grey Bebout and an anonymous reviewer who substantially improved this manuscript. Sarah Penniston-Dorland is thanked for both the helpful comments and editorial handling.

DATA AVAILABILITY STATEMENT

The data that support the findings of this study are available in the supplementary material of this article.

ORCID

F. Zeb Page https://orcid.org/0000-0002-2100-0806

REFERENCES

Anczkiewicz, R., Platt, J. P., Thirlwall, M., & Wakabayashi, J. (2004). Franciscan subduction off to a slow start: Evidence from high-precision Lu–Hf garnet ages on high grade-blocks. *Earth and Planetary Science Letters*, *225*, 147–161. https://doi.org/10.1016/j.epsl.2004.06.003

Bailey, E. H., Irwin, W. P., & Jones, D. L. (1964). *Franciscan and related rocks, and their significance in the geology of western California*. California Division of Mines and Geology Bulletin.

Bebout, G. E., & Barton, M. (1989). Fluid flow and metasomatism in a subduction zone hydrothermal system; Catalina schist terrane. *Geology*, *17*, 976–980.

Bebout, G. E., & Penniston-Dorland, S. C. (2016). Fluid and mass transfer at subduction interfaces—The field metamorphic record. *Lithos*, *240-243*, 228–258. https://doi.org/10.1016/j.lithos.2015.10.007

Blanco-Quintero, I., García-Casco, A., & Gerya, T. V. (2011). Tectonic blocks in serpentinite mélange (eastern Cuba) reveal large-scale convective flow of the subduction channel. *Geology*, *39*, 79–82. https://doi.org/10.1130/G31494.1

Bonamici, C. E., Kozdon, R., Ushikubo, T., & Valley, J. W. (2011). High-resolution P-T-t paths from $\delta^{18}O$ zoning in titanite: A snapshot of late-orogenic collapse in the Grenville of New York. *Geology*, *39*, 959–962. https://doi.org/10.1130/G32130.1

Bonamici, C. E., Kozdon, R., Ushikubo, T., & Valley, J. W. (2014). Intragrain oxygen isotope zoning in titanite by SIMS: Cooling rates and fluid infiltration along the Carthage-Colton mylonite zone, Adirondack Mountains, NY, USA. *Journal of Metamorphic Geology*, *32*, 71–92. https://doi.org/10.1111/jmg.12059

Borg, I. Y. (1956). Glaucophane schists and eclogites near Healdsburg, California. *Geological Society of America Bulletin*, *67*, 1563–1584. https://doi.org/10.1130/0016-7606(1956)67[1563:GSAENH]2.0.CO;2

Bovay, T., Rubatto, D., & Lanari, P. (2021). Pervasive fluid-rock interaction in subducted oceanic crust revealed by oxygen isotope zoning in garnet. *Contributions to Mineralogy and Petrology*, *176*, 55. https://doi.org/10.1007/s00410-021-01806-4

Bruand, E., Storey, C. D., Fowler, M., Heilimo, E., & EIMF. (2019). Oxygen isotopes in titanite and apatite, and their potential for crustal evolution research. *Geochimica et Cosmochimica Acta*, *255*, 144–162. https://doi.org/10.1016/j.gca.2019.04.002

Cavosie, A. J., Valley, J. W., Wilde, S. A., & EIMF. (2005). Magmatic $\delta^{18}O$ in 4400–3900 Ma detrital zircons: A record of the alteration and recycling of crust in the Early Archean. *Earth and Planetary Science Letters*, *235*, 663–681. https://doi.org/10.1016/j.epsl.2005.04.028

Cisneros, M., Behr, W. M., Platt, J. P., & Anczkiewicz, R. (2022). Quartz-in-garnet barometry constraints on formation pressures of eclogites from the Franciscan Complex, California. *Contributions to Mineralogy and Petrology*, *177*, 12. https://doi.org/10.1007/s00410-021-01876-4

Cloos, M. (1982). Flow melanges: Numerical modeling and geologic constraints on their origin in the Franciscan subduction complex, California. *Geological Society of America Bulletin*, *93*, 330–345. https://doi.org/10.1130/0016-7606(1982)93<330:FMNMAG>2.0.CO;2

Coleman, R. G., & Lee, D. E. (1963). Glaucophane-bearing metamorphic rock types of the Cazadero area, California. *Journal of Petrology*, *4*, 260–301. https://doi.org/10.1093/petrology/4.2.260

Cruz-Uribe, A. M., Feineman, M. D., Zack, T., & Jacob, D. E. (2018). Assessing trace element (dis)equilibrium and the application of single element thermometers in metamorphic rocks. *Lithos*, *314-315*, 1–15. https://doi.org/10.1016/j.lithos.2018.05.007

Cruz-Uribe, A. M., Page, F. Z., Lozier, E., Feineman, M. D., Zack, T., Mertz-Kraus, R., Jacob, D. E., & Kitajima, K. (2021). Trace element and isotopic zoning of garnetite veins in amphibolitized eclogite, Franciscan Complex, California, USA. *Contributions to Mineralogy and Petrology*, *176*, 1–19.

Ernst, W. G. (1970). Tectonic contact between the Franciscan mélange and the Great Valley sequence—Crustal expression of a late Mesozoic Benioff zone. *Journal of Geophysical Research*, *75*, 886–901. https://doi.org/10.1029/JB075i005p00886

Errico, J. C., Barnes, J. D., Strickland, A., & Valley, J. W. (2013). Oxygen isotope zoning in garnets from Franciscan eclogite blocks: Evidence for rock-buffered fluid interaction in the mantle wedge. *Contributions to Mineralogy and Petrology*, *166*, 1161–1176. https://doi.org/10.1007/s00410-013-0915-0

Essene, E. J., & Fyfe, W. S. (1967). Omphacite in Californian metamorphic rocks. *Contributions to Mineralogy and Petrology*, *15*, 1–23. https://doi.org/10.1007/BF01167213

Garber, J. M., Hacker, B. R., Kylander-Clark, A. R. C., Stearns, M., & Seward, G. (2017). Controls on trace element uptake in metamorphic titanite: Implications for petrochronology. *Journal of Petrology*, *58*, 1031–1057. https://doi.org/10.1093/petrology/egx046

Gealy, W. K. (1951). Geology of the Healdsburg quadrangle, California. *California Division of Mines and Geology Bulletin*, *161*, 7–50.

Goltz, A. E. (2017). *Tracing fluids: Microanalysis of four Franciscan garnets*. Oberlin.

Goltz, A. E., Hoover, W. F., Page, F. Z., Moreira, H., Storey, C.D., Kitajima, K., & Valley, J. W. (2017). Microanalyzing metasomatism: Correlative microanalysis of trace elements and oxygen isotopes in the Franciscan. In: Presented at the AGU Fall Meeting Abstracts, New Orleans.

Goltz, A. E., & Page, F. Z. (2016). Mingled metamorphism: Computational modelling of an oxidized Franciscan blueschist-eclogite and implications for metamorphic evolutionary models. In: Presented at the GSA Annual Meeting in Denver, Colorado, USA - 2016, Geological Society of America. https://doi.org/10.1130/abs/2016AM-282106

Gregory, R. T., & Taylor, H. P. (1981). An oxygen isotope profile in a section of Cretaceous oceanic crust, Samail ophiolite, Oman: Evidence for $\delta^{18}O$ buffering of the oceans by deep (>5 km) seawater-hydrothermal circulation at mid-ocean ridges. *Journal of Geophysical Research - Solid Earth*, *86*, 2737–2755. https://doi.org/10.1029/JB086iB04p02737

Hayden, L., Watson, E., & Wark, D. (2008). A thermobarometer for sphene (titanite). *Contributions to Mineralogy and Petrology*, *155*, 529–540.

Hermes, O. D. (1973). Paragenetic relationships in an amphibolitic tectonic block in the Franciscan terrain, Panoche Pass, California. *Journal of Petrology*, *14*, 1–32. https://doi.org/10.1093/petrology/14.1.1

Hoover, W. F. (2014). *Eclogites and eclogites: Oxygen isotope evidence of a shared subduction origin for Franciscan eclogites and Moses rock eclogite xenoliths*. Oberlin College.

Horodyskyj, U., Lee, C.-T. A., & Luffi, P. (2009). Geochemical evidence for exhumation of eclogite via serpentinite channels in ocean–continent subduction zones. *Geosphere*, *5*, 426–438. https://doi.org/10.1130/GES00502.1

Jochum, K. P., Weis, U., Stoll, B., Kuzmin, D., Yang, Q., Raczek, I., Jacob, D. E., Stracke, A., Birbaum, K., Frick, D. A., Günther, D., & Enzweiler, J. (2011). Determination of reference values for NIST SRM 610–617 glasses following ISO guidelines. *Geostandards Newsletter*, *35*, 397–429. https://doi.org/10.1111/j.1751-908X.2011.00120.x

Kohn, M. J. (2017). Titanite petrochronology. *Reviews in Mineralogy and Geochemistry*, *83*, 419–441. https://doi.org/10.2138/rmg.2017.83.13

Konrad-Schmolke, M., Halama, R., Chew, D., Heuzé, C., De Hoog, J., & Ditterova, H. (2022). Discrimination of thermodynamic and kinetic contributions to the heavy rare earth element patterns in metamorphic garnet. *Journal of Metamorphic Geology*. https://doi.org/10.1111/jmg.12703

Konrad-Schmolke, M., Zack, T., O'Brien, P. J., & Jacob, D. (2008). Combined thermodynamic and rare earth element modelling of garnet growth during subduction: Examples from ultrahigh-pressure eclogite of the Western Gneiss Region, Norway. *Earth and Planetary Science Letters*, *272*, 488–498. https://doi.org/10.1016/j.epsl.2008.05.018

Krogh, E. J., Oh, C.-W., & Liou, J. G. (1994). Polyphase and anticlockwise P–T evolution for Franciscan eclogites and blueschists from Jenner, California, USA. *Journal of Metamorphic Geology*, *12*, 121–134. https://doi.org/10.1111/j.1525-1314.1994.tb00008.x

Krogh Ravna, E. J., & Terry, M. P. (2004). Geothermobarometry of UHP and HP eclogites and schists—An evaluation of equilibria among garnet-clinopyroxene-kyanite-phengite-coesite/-quartz. *Journal of Metamorphic Geology*, *22*, 579–592. https://doi.org/10.1111/j.1525-1314.2004.00534.x

Krohe, A. (2017). The Franciscan Complex (California, USA)—The model case for return-flow in a subduction channel put to the test. *Gondwana Research*, *45*, 282–307. https://doi.org/10.1016/j.gr.2017.02.003

Luvizotto, G. L., & Zack, T. (2009). Nb and Zr behavior in rutile during high-grade metamorphism and retrogression: An example from the Ivrea–Verbano Zone. *Chemical Geology*, *261*, 303–317. https://doi.org/10.1016/j.chemgeo.2008.07.023

Martin, L. A. J., Rubatto, D., Crépisson, C., Hermann, J., Putlitz, B., & Vitale Brovarone, A. (2014). Garnet oxygen analysis by SHRIMP-SI: Matrix corrections and application to high-pressure metasomatic rocks from Alpine Corsica. *Chemical Geology*, *374-375*, 25–36. https://doi.org/10.1016/j.chemgeo.2014.02.010

Matthews, A. (1994). Oxygen isotope geothermometers for metamorphic rocks. *Journal of Metamorphic Geology*, *12*, 211–219. https://doi.org/10.1111/j.1525-1314.1994.tb00017.x

Meinhold, G., Anders, B., Kostopoulos, D., & Reischmann, T. (2008). Rutile chemistry and thermometry as provenance indicator: An example from Chios Island, Greece. *Sedimentary Geology*, *203*, 98–111. https://doi.org/10.1016/j.sedgeo.2007.11.004

Moore, D., Cherniak, D., & Watson, E. (1998). Oxygen diffusion in rutile from 750 to 1000 degrees C and 0.1 to 1000 MPa. *American Mineralogist*, *83*, 700–711. https://doi.org/10.2138/am-1998-7-803

Moore, D. E. (1984). Metamorphic history of a high-grade blueschist exotic block from the Franciscan Complex, California. *Journal of Petrology*, *25*, 126–150. https://doi.org/10.1093/petrology/25.1.126

Moore, D. E., & Blake, M. C. (1989). New evidence for polyphase metamorphism of glaucophane schist and eclogite exotic blocks in the Franciscan Complex, California and Oregon. *Journal of Metamorphic Geology*, *7*, 211–228. https://doi.org/10.1111/j.1525-1314.1989.tb00585.x

Mulcahy, S. R., Starnes, J. K., Day, H. W., Coble, M. A., & Vervoort, J. (2018). Early onset of Franciscan subduction. *Tectonics*, *37*, 1194–1209. https://doi.org/10.1029/2017TC004753

Oh, C.-W., Liou, J. G., & Maruyama, S. (1991). Low-temperature eclogites and eclogitic schists in Mn-rich metabasites in Ward Creek, California; Mn and Fe effects on the transition between blueschist and eclogite. *Journal of Petrology*, *32*, 275–302. https://doi.org/10.1093/petrology/32.2.275

Page, F. Z., Armstrong, L., Essene, E. J., & Mukasa, S. B. (2007). Prograde and retrograde history of the Junction School eclogite, California, and an evaluation of garnet–phengite–clinopyroxene thermobarometry. *Contributions to Mineralogy and Petrology*, *153*, 533–555. https://doi.org/10.1007/s00410-006-0161-9

Page, F. Z., Cameron, E. M., Flood, C. M., Dobbins, J. W., Spicuzza, M. J., Kitajima, K., Strickland, A., Ushikubo, T.,

Mattinson, C. G., & Valley, J. W. (2019). Extreme oxygen isotope zoning in garnet and zircon from a metachert block in mélange reveals metasomatism at the peak of subduction metamorphism. *Geology*, *47*(7), 655–658.

Page, F. Z., Essene, E. J., Mukasa, S. B., & Valley, J. W. (2014). A garnet-zircon oxygen isotope record of subduction and exhumation fluids from the Franciscan Complex, California. *Journal of Petrology*, *55*, 103–131. https://doi.org/10.1093/petrology/egt062

Pearce, N. J. G., Perkins, W. T., Westgate, J. A., Gorton, M. P., Jackson, S. E., Neal, C. R., & Chenery, S. P. (1997). A compilation of new and published major and trace element data for NIST SRM 610 and NIST SRM 612 glass reference materials. *Geostandards Newsletter*, *21*, 115–144. https://doi.org/10.1111/j.1751-908X.1997.tb00538.x

Pereira, I., Storey, C. D., Darling, J., Lana, C., & Alkmim, A. R. (2019). Two billion years of evolution enclosed in hydrothermal rutile: Recycling of the São Francisco Craton Crust and constraints on gold remobilisation processes. *Gondwana Research*, *68*, 69–92. https://doi.org/10.1016/j.gr.2018.11.008

Raymond, L. A. (2017). A metasomatic setting, the Russian River Arch, and gravitational emplacement in the history of eclogites at the classic eclogite locality of Jenner, California, USA. *International Geology Review*, *59*, 577–598. https://doi.org/10.1080/00206814.2016.1213143

Rubatto, D., & Angiboust, S. (2015). Oxygen isotope record of oceanic and high-pressure metasomatism: A P–T–time–fluid path for the Monviso eclogites (Italy). *Contributions to Mineralogy and Petrology*, *170*(44), 1–16.

Russell, A. K., Kitajima, K., Strickland, A., Medaris, L. G., Schulze, D. J., & Valley, J. W. (2013). Eclogite-facies fluid infiltration: Constraints from δ18O zoning in garnet. *Contributions to Mineralogy and Petrology*, *165*(1), 103–116.

Rutte, D., Garber, J., Kylander-Clark, A., & Renne, P. R. (2020). An exhumation pulse from the nascent Franciscan subduction zone (California, USA). *Tectonics*, *39*(10), e2020TC006305. https://doi.org/10.1029/2020tc006305

Sorensen, S. S., Grossman, J., & Perfit, M. (1997). Phengite-hosted LILE enrichment in eclogite and related rocks: Implications for fluid-mediated mass transfer in subduction zones and arc magma genesis. *Journal of Petrology*, *38*, 3–34. https://doi.org/10.1093/petroj/38.1.3

Switzer, G. (1945). Eclogite from the California glaucophane schists. *American Journal of Science*, *243*, 1–8. https://doi.org/10.2475/ajs.243.1.1

Taylor, R., Clark, C., & Reddy, S. M. (2012). The effect of grain orientation on secondary ion mass spectrometry (SIMS) analysis of rutile. *Chemical Geology*, *300-301*, 81–87. https://doi.org/10.1016/j.chemgeo.2012.01.013

Tomkins, H. S., Powell, R., & Ellis, D. (2007). The pressure dependence of the zirconium-in-rutile thermometer. *Journal of Metamorphic Geology*, *25*, 703–713. https://doi.org/10.1111/j.1525-1314.2007.00724.x

Tsujimori, T., Matsumoto, K., Wakabayashi, J., & Liou, J. G. (2006). Franciscan eclogite revisited: Reevaluation of the P–T evolution of tectonic blocks from Tiburon Peninsula, California, U.S.A. *Mineralogy and Petrology*, *88*, 243–267. https://doi.org/10.1007/s00710-006-0157-1

Ukar, E., & Cloos, M. (2016). Graphite-schist blocks in the Franciscan Mélange, San Simeon, California: Evidence of high-P metamorphism. *Journal of Metamorphic Geology*, *34*, 191–208. https://doi.org/10.1111/jmg.12174

Valley, J. W., Bindeman, I. N., & Peck, W. H. (2003). Empirical calibration of oxygen isotope fractionation in zircon. *Geochimica et Cosmochimica Acta*, *67*, 3257–3266. https://doi.org/10.1016/S0016-7037(03)00090-5

Vho, A., Lanari, P., & Rubatto, D. (2019). An internally-consistent database for oxygen isotope fractionation between minerals. *Journal of Petrology*, *60*, 2101–2129. https://doi.org/10.1093/petrology/egaa001

Vho, A., Lanari, P., Rubatto, D., & Hermann, J. (2020). Tracing fluid transfers in subduction zones: An integrated thermodynamic and δ18O fractionation modelling approach. *Solid Earth*, *11*, 307–328. https://doi.org/10.5194/se-11-307-2020

Viete, D. R., Hacker, B. R., Allen, M. B., Seward, G. G. E., Tobin, M. J., Kelley, C. S., Cinque, G., & Duckworth, A. R. (2018). Metamorphic records of multiple seismic cycles during subduction. *Science Advances*, *4*, eaaq0234. https://doi.org/10.1126/sciadv.aaq0234

Wakabayashi, J. (2015). Anatomy of a subduction complex: Architecture of the Franciscan Complex, California, at multiple length and time scales. *International Geology Review*, *57*, 669–746. https://doi.org/10.1080/00206814.2014.998728

Wakabayashi, J. (2012). Subducted sedimentary serpentinite mélanges: Record of multiple burial–exhumation cycles and subduction erosion. *Tectonophysics*, *568-569*, 230–247. https://doi.org/10.1016/j.tecto.2011.11.006

Wakabayashi, J. (1990). Counterclockwise P-T-t paths from amphibolites, Franciscan Complex, California: Relics from the early stages of subduction zone metamorphism. *The Journal of Geology*, *98*, 657–680. https://doi.org/10.2307/30068037?refreqid=search-gateway:1c411e6f325cb4a1085ec0e346afa547

Walters, J. B., Cruz-Uribe, A. M., Song, W. J., Gerbi, C., & Biela, K. (2022). Strengths and limitations of in situ U–Pb titanite petrochronology in polymetamorphic rocks: An example from western Maine, USA. *Journal of Metamorphic Geology*, *40*, 1043–1066. https://doi.org/10.1111/jmg.12657

Whitney, D. L., & Evans, B. W. (2009). Abbreviations for names of rock-forming minerals. *American Mineralogist*, *95*, 185–187. https://doi.org/10.2138/am.2010.3371

Zack, T., von Eynatten, H., & Kronz, A. (2004). Rutile geochemistry and its potential use in quantitative provenance studies. *Sedimentary Geology*, *171*, 37–58. https://doi.org/10.1016/j.sedgeo.2004.05.009

Zack, T., & Kooijman, E. (2017). Petrology and geochronology of rutile. *Reviews in Mineralogy and Geochemistry*, *83*, 443–467. https://doi.org/10.2138/rmg.2017.83.14

Zhang, X. Y., Cherniak, D. J., & Watson, E. B. (2006). Oxygen diffusion in titanite: Lattice diffusion and fast-path diffusion in single crystals. *Chemical Geology*, *235*, 105–123. https://doi.org/10.1016/j.chemgeo.2006.06.005

SUPPORTING INFORMATION

Additional supporting information can be found online in the Supporting Information section at the end of this article.

Table S1. SIMS oxygen isotope data for rutile.

Table S2. SIMS oxygen isotope data for titanite, including calibration curves for compositional bias.

Table S3. Secondary SRMs for quality control in LA-ICPMS analyses. N.A. - not analysed, N.D. - not detected.

Table S4. Correlated major, trace element and oxygen isotope data for Franciscan rutile and titanite. NA = Not analysed.

Figure S5. Supporting information.

How to cite this article: Page, F. Z., Storey, C. D., & EIMF (2023). A rutile and titanite record of subduction fluids: Integrated oxygen isotope and trace element analyses in Franciscan high-pressure rocks. *Journal of Metamorphic Geology*, *41*(6), 767–786. https://doi.org/10.1111/jmg.12717